

Structures of Niobium and Tantalum Oxide Fluorides Containing Lone-Pair Ions

IV. $\text{Pb}_{12}\text{Ta}_9\text{O}_{20}\text{F}_{29}$: A "Block" Structure Related to the Aurivillius Phases

ÖRJAN SÄVBORG

*Department of Inorganic Chemistry, Arrhenius Laboratory,
University of Stockholm, S-106 91 Stockholm, Sweden*

Received December 30, 1983

The crystal structure of the compound $\text{Pb}_{12}\text{Ta}_9\text{O}_{20}\text{F}_{29}$ has been determined from single crystal X-ray data. The symmetry is tetragonal (space group $I4/m$) with the unit cell dimensions $a = 22.8951(6)$ Å and $c = 3.9202(2)$ Å. The structure contains columns of ReO_3 structure type, 3×3 octahedra wide, separated by " $\text{Pb}_2\text{F}_2^{2+}$ " layers. It is thus related to the structures of the layered $\text{Bi}_2\text{O}_2^{2+}$ perovskites, the so-called Aurivillius phases. Most of the fluorine atoms in the structure have been located by means of bond strength calculations. © 1985 Academic Press, Inc.

Introduction

Phase analysis studies of the system $\text{Pb(II)}\text{--Nb(V)}\text{--O--F}$ have established the existence of a compound $\text{Pb}_2\text{Nb}_3\text{O}_7\text{F}_5$, which, from a single crystal structure determination, has been shown to be related to the Aurivillius phases (1). An investigation of the $\text{Pb(II)}\text{--Ta(V)}\text{--O--F}$ system indicated the existence of several new phases, such as $\text{Pb}_3\text{Ta}_5\text{O}_9\text{F}_{13}$ (2), $\text{Pb}_{0.24}\text{Ta}(\text{O},\text{F})_{3.12}$ (3), and a phase with the gross composition $\text{Pb}_{0.57}\text{Ta}_{0.43}\text{O}_{0.95}\text{F}_{1.39}$. The X-ray powder pattern from the latter phase, although more complex, showed some similarities to the pattern of $\text{Pb}_2\text{Nb}_3\text{O}_7\text{F}_5$. It is also worth noticing that both compounds decompose when heated in sealed Pt capsules above 900 K. A single crystal X-ray structure analysis of the tantalum compound was performed to clarify the possible structural relationship between these two phases, and the results are reported in the present paper.

Experimental

Samples for the phase analysis were prepared by heat treatment of appropriate mixtures of PbF_2 , PbO , TaO_2F , and Ta_2O_5 in closed Pt ampoules for 1 week at various temperatures. The products were characterized by their X-ray powder patterns, recorded in a Guinier–Hägg focusing camera with KCl ($a = 6.2930$ Å at 298 K) (4) added as an internal standard. A sample, with the gross composition $\text{Pb}_{0.57}\text{Ta}_{0.43}\text{O}_{0.95}\text{F}_{1.39}$, prepared at 875 K, gave a powder pattern which could be fully indexed on the basis of a body centered tetragonal unit cell with $a = 22.895$ Å and $c = 3.9202$ Å (cf. Table I). It consisted of very thin colorless needles with the c axis parallel to the needle axis. These were too small for single crystal X-ray diffraction data collection. Several unsuccessful attempts were made to increase the crystal size by longer heating times—up to 4 weeks—with intermittent regrinding. A multiphase sample containing less PbF_2

TABLE I
CRYSTALLOGRAPHIC DATA FOR $\text{Pb}_{12}\text{Ta}_9\text{O}_{20}\text{F}_{29}$

hkl	$2\theta_{\text{obs}}$ ($^{\circ}$)	$\Delta 2\theta$ ($^{\circ}$)	d_{obs} (\AA)	I/I_0
1 1 0	5.498	0.044	16.062	17
2 0 0	7.761	0.044	11.382	18
3 3 0	16.435	0.022	5.389	7
4 2 0	17.323	0.015	5.115	22
5 1 0	19.780	0.023	4.485	15
4 4 0	21.967	0.024	4.043	35
5 3 0	22.640	0.013	3.9243	155
1 0 1	23.004	0.006	3.8631	175
6 0 0	23.307	0.015	3.8135	76
2 1 1	24.312	0.020	3.6581	154
6 2 0	24.588	0.016	3.6176	351
3 2 1	26.712	0.009	3.3347	511
7 1 0	27.529	0.003	3.2375	763
6 4 0	28.089	0.007	3.1742	195
5 0 1	29.980	-0.002	2.9781	1000
5 2 1	31.019	0.015	2.8808	30
8 0 0	31.236	0.008	2.8612	33
8 2 0	32.221	-0.004	2.7760	21
6 6 0	33.184	0.008	2.6976	29
7 5 0	33.650	0.003	2.6613	131

$M(20) = 35; F(20) = 46$

($\text{Pb}_{0.375}\text{Ta}_{0.625}\text{O}_{1.46}\text{F}_{0.955}$), prepared at the same temperature, did, however, contain some rod-shaped crystals that gave an identical powder pattern. The crystals were white but usually not fully transparent, indicating that they were of poor quality, which was also confirmed by Weissenberg photographs. An almost transparent crystal with fairly well-developed faces was finally found; and it yielded Weissenberg photographs with sharp diffraction spots. This crystal was mounted on a PW 1100 automatic four-circle diffractometer and used

for intensity data collection. Relevant data on the crystal and data collection are given in Table II. Scattering factors and anomalous scattering parameters were taken from (5).

Structure Determination

The Weissenberg photographs showed the Laue symmetry to be $4/m$. Only reflections obeying the condition $h + k + l = 2n$ were observed, thus limiting the possible space groups to $I4$ (No. 79), $I4$ (No. 82) and $I4/m$ (No. 87). Since statistical tests indicated a centrosymmetric space group, the $I4/m$ symmetry was initially assumed.

Figure 1a shows a HREM structure image taken with a Siemens Elmiscop, operated at 125 kV, and with the electron beam parallel to $[001]$. In this picture groups of four light spots arranged as squares could be seen, and these were interpreted as the four tunnels within a column consisting of $3 \times 3 \times \infty$ octahedra (cf. Fig. 1). A close inspection of the picture revealed that the square groups are rotated around $[001]$ through an angle of approximately 7° relative to a perfectly linear arrangement of the columns. Assuming all diagonals of TaX_6 ($X = \text{O}, \text{F}$) octahedra to have the same size as the c axis, preliminary Ta coordinates were

TABLE II
DETAILS OF DATA COLLECTION

Crystal size	$0.028 \times 0.028 \times 0.136 \text{ mm}^3$
Radiation	$\text{MoK}\alpha, \lambda = 0.7101 \text{ \AA}$
Absorption coefficient	$\mu = 733.6 \text{ cm}^{-1}$
Transmission factors	0.114–0.197
Scan type	$\theta-2\theta$
Scan speed	$0.02^{\circ} \text{ sec}^{-1}$
Scan width	$\pm 1.1^{\circ}$
Number of registered reflections	1490
Number of reflections with $I > 2.5\sigma(I)$ used in least-squares refinement	885

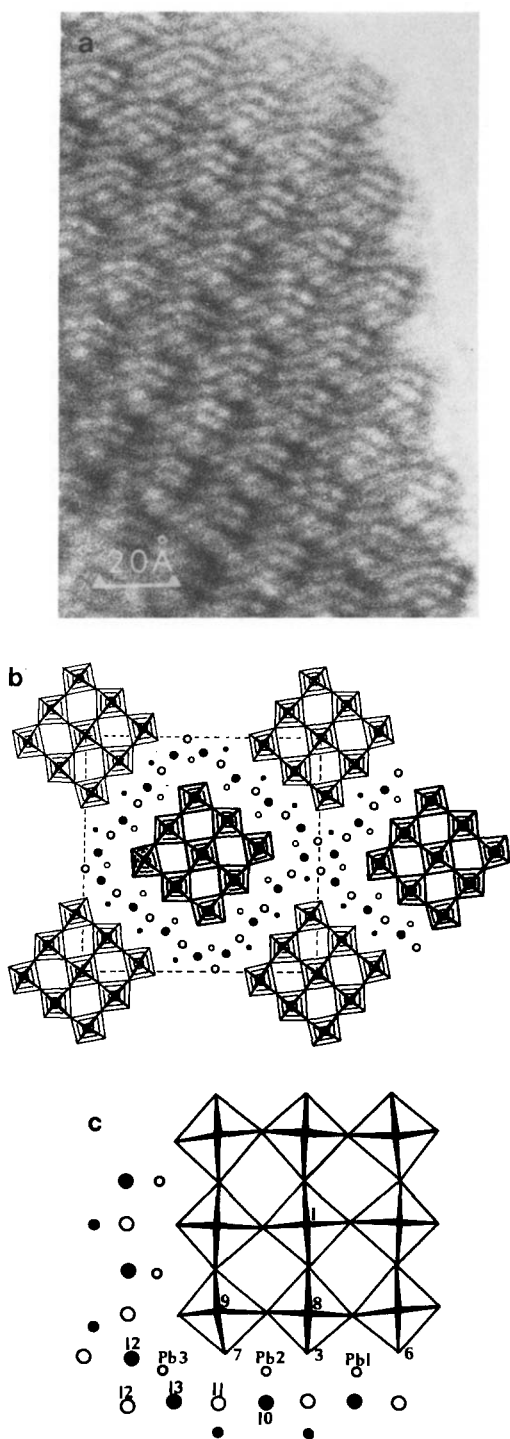


FIG. 1. (a) An HREM image of $\text{Pb}_{12}\text{Ta}_9\text{O}_{20}\text{F}_{29}$ taken with the electron beam parallel to $[001]$. (b) The struc-

derived for this structure model. These were used to calculate an observed Fourier map, which yielded reasonable Pb atom positions corresponding to the expected Pb/Ta ratio. A difference Fourier map located a number of anions corresponding to the preliminary composition. Least-squares refinement of this structure model, with isotropic thermal parameters for all atoms and with all anions treated as oxygens, resulted in an R value of 0.082. A subsequent difference map indicated that the thermal motion of the Ta atoms was anisotropic. A refinement with anisotropic thermal parameters for all metal atoms converged to $R = 0.064$.

Trial refinements in the other two possible space groups did not lower the R value or cause significant shifts in the atom positions. The final positional and thermal parameters are given in Table III and the relevant interatomic distances are summarized in Table IV.

The composition of this structure model, depicted in Fig. 1b, is $\text{Pb}_{12}\text{Ta}_9\text{X}_{49}$. Due to the small difference in scattering power it is almost impossible to determine whether a site is occupied by oxygen or fluorine when using X-ray data to refine heavy atom structures. The compound is colorless, however, which implies that the oxidation states of the metal atoms are strictly Pb(II) and Ta(V). The requirement of electrical neutrality then yields the composition $\text{Pb}_{12}\text{Ta}_9\text{O}_{20}\text{F}_{29}$. Attempts to refine the structure with different distributions of O and F atoms were unsuccessful, since no significant change was observed in either the R value or the standard deviations of the anion coordinates.

In previous structure determinations of

ture of $\text{Pb}_{12}\text{Ta}_9\text{O}_{20}\text{F}_{29}$ projected along $[001]$. Octahedra in fine and bold lines have their Ta atoms at $z = 0$ and $z = \frac{1}{2}$, respectively. Large circles = F atoms, small circles = Pb atoms at $z = 0$ (unfilled), and $z = \frac{1}{2}$ (filled). (c) An enlarged section of b showing the numbering of atoms.

TABLE III
THE FINAL POSITIONAL AND THERMAL PARAMETERS FOR Pb₁₂Ta₉O₂₀F₂₉ $z = 0$ FOR ALL ATOMS

Atom	Position	<i>x</i>	<i>y</i>	<i>U</i> or <i>U</i> ₁₁ ^a	<i>U</i> ₂₂	<i>U</i> ₃₃	<i>U</i> ₁₂
Pb(1)	8(<i>h</i>)	0.3951(1)	0.2111(1)	179(11)	142(10)	115(11)	3(8)
Pb(2)	8(<i>h</i>)	0.2554(1)	0.3280(1)	178(11)	186(11)	180(13)	-24(9)
Pb(3)	8(<i>h</i>)	0.1018(1)	0.4529(1)	135(10)	246(12)	141(12)	-21(9)
Ta(1)	2(<i>a</i>)	0	0	71(12)	71(12)	183(26)	0
Ta(2)	8(<i>h</i>)	0.2329(1)	0.0290(1)	76(10)	62(9)	123(12)	-4(8)
Ta(3)	8(<i>h</i>)	0.1011(1)	0.1306(1)	61(9)	55(9)	231(14)	1(8)
X(1)	2(<i>b</i>)	$\frac{1}{2}$	$\frac{1}{2}$	139(187)			
X(2)	8(<i>h</i>)	0.049(2)	0.069(2)	234(110)			
X(3)	8(<i>h</i>)	0.156(2)	0.200(2)	146(96)			
X(4)	8(<i>h</i>)	0.172(3)	0.086(3)	343(139)			
X(5)	8(<i>h</i>)	0.044(3)	0.197(3)	430(168)			
X(6)	8(<i>h</i>)	0.018(2)	0.310(2)	53(77)			
X(7)	8(<i>h</i>)	0.289(2)	0.100(2)	189(102)			
X(8)	8(<i>h</i>)	0.393(2)	0.358(2)	145(109)			
X(9)	8(<i>h</i>)	0.527(2)	0.257(2)	69(82)			
X(10)	8(<i>h</i>)	0.285(1)	0.226(1)	-97(66)			
X(11)	8(<i>h</i>)	0.146(2)	0.331(2)	156(96)			
X(12)	8(<i>h</i>)	0.564(2)	0.004(2)	-6(67)			
X(13)	8(<i>h</i>)	0.423(2)	0.112(2)	102(82)			

^a Anisotropic temperature factors are given in the form $\exp\{-2\pi^2 \cdot 10^{-4} (h^2a^{*2}U_{11} + k^2b^{*2}U_{22} + l^2c^{*2}U_{33} + kha^*b^*U_{12})\}$.

oxide fluorides (1, 2, 6) the fluorines were located by means of "bond strength sums" for all Pb–X and Ta–X bonds, evaluated with the parameters for metal–oxygen bonds given by Brown and Kang (7). The results of such calculations for the present compound are summarized in Table V. They indicate that the X(3), X(6–7), and X(10–13) positions are fully occupied by fluorine, accounting for 56 of the 58 fluorine atoms in the unit cell. The only twofold anion position in the structure is X(1) but the bond strength calculations do not support the location of fluorine at this position.

Description

A projection of the structure of Pb₁₂Ta₉O₂₀F₂₉ along [001] is shown in Fig. 1b. It consists of infinite columns of ReO₃ structure type, 3 × 3 octahedra wide and with the net composition Ta₉X₃₃, running parallel to [001]. The columns are separated

from each other by PbX layers with the net composition Pb₉X₁₆, running parallel to {340}. Alternate columns along <110> are displaced by $\tilde{c}/2$ relative to each other. The columns are slightly rotated anticlockwise around [001] so that their edges make an angle of 7° with the <110> directions.

The columns are built up from three crystallographically different Ta atoms, all of which are octahedrally surrounded by X atoms. The TaX₆ octahedra are all quite regular, with an average Ta–X distance of 1.96 Å in fair agreement with 1.92 Å in TaO₂F (8). The deviations from perfectly regular coordination in the Ta(2) and Ta(3) octahedra are caused by a small shift toward the PbX layers of the anions facing the layers; this effect is also observed in Pb₂Nb₃O₇F₅ (1).

The structure contains three crystallographically independent lead atoms. Two of these are surrounded by eight fluorine atoms at the corners of a deformed square

TABLE IV
SELECTED INTERATOMIC
DISTANCES FOR $\text{Pb}_{12}\text{Ta}_9\text{O}_{20}\text{F}_{29}$
IN Å

Ta(1)–X(2)	4 ×	1.94(5)
X(1)	2 ×	1.96(1)
Ta(2)–X(5)		1.85(7)
X(4)		1.90(6)
X(6)		2.06(4)
X(7)		2.07(5)
X(9)	2 ×	1.97(1)
Ta(3)–X(2)		1.84(6)
X(4)		1.92(6)
X(5)		2.01(7)
X(3)		2.02(4)
X(8)	2 ×	1.98(1)
Pb(1)–X(13)		2.35(4)
X(11)	2 ×	2.37(3)
X(10)		2.55(3)
X(6)		2.83(3)
X(3)	2 ×	3.07
Pb(2)–X(10)		2.44(3)
X(10)	2 ×	2.49(2)
X(11)		2.51(5)
X(7)	2 ×	2.76(4)
X(3)	2 ×	2.88(3)
Pb(3)–X(12)		2.26(3)
X(12)	2 ×	2.44(2)
X(13)	2 ×	2.53(3)
X(13)		2.85(4)
X(11)		2.97(5)
(X–X) _{min}		2.56(8)

antiprism, an arrangement very similar to that found in $\text{Pb}_2\text{Nb}_3\text{O}_7\text{F}_5$ (1). Four lead atoms of the third type make up the intersection of the PbX layers. These atoms have a somewhat different coordination. They are bonded to five X anions arranged as a square pyramid with the lead atom a short distance outside the base. The shortest Pb(3)–X distance is across this base plane. A similar coordination has been observed in $\text{Pb}_3\text{Nb}_4\text{O}_{12}\text{F}_2$ (6) and also in BrF_5 (9), IF_5 (10), and XeF_6 (11). It has been attributed to the repulsion of the highly electronegative ligands by the lone-pair electrons on the central atom (12).

In the crystal structure of each of the three compounds $\text{Pb}_2\text{Nb}_3\text{O}_7\text{F}_5$ (1), Pb_3Ta_5

O_9F_{13} (2), and $\text{Pb}_{12}\text{Ta}_9\text{O}_{20}\text{F}_{29}$, two building elements can be discerned. One of these is a slab or column of corner-sharing MX_6 octahedra arranged as in ReO_3 . The other is a layer or band of PbX with an atomic arrangement similar to that in tetragonal PbO (13). The ReO_3 -type elements are not directly bonded to each other but are interleaved with PbX elements. However, none of the three compounds has an X–Pb–X link with short Pb–X bonds (<2.5 Å) between the ReO_3 -type elements. The force binding slabs (columns) together thus seems to be mainly an electrostatic attraction to the PbX element. This means, however, that the PbX element must carry a net charge. Consequently, the X atoms in the PbX layer must be mainly of F^- character and the layers must be “ $\text{Pb}_2\text{F}_2^{2+}$ ” as indicated by the bond strength calculations.

TABLE V
BOND STRENGTH SUMS FOR $\text{Pb}_{12}\text{Ta}_9\text{O}_{20}\text{F}_{29}$
CALCULATED WITH PARAMETERS
FROM REF. (7)

Atom	ΣS_{calc}	Suggested anion character
Ta(1)	5.44	
Ta(2)	5.13	
Ta(3)	5.31	
Pb(1)	2.43	
Pb(2)	2.37	
Pb(3)	2.40	
X(1)	1.74	
X(2)	2.10	O
X(3)	1.25	F
X(4)	2.12	O
X(5)	2.07	O
X(6)	1.17	F
X(7)	1.05	F
X(8)	1.73	
X(9)	1.84	
X(10)	1.35	F
X(11)	1.32	F
X(12)	1.31	F
X(13)	1.24	F

Discussion

Structures built up from ReO_3 -type slabs separated by crystallographic shear planes are a well-known feature of the molybdenum and tungsten oxides. Two such niobium phases are also known, viz., $R\text{-Nb}_2\text{O}_5$ (14) and $\text{Nb}_3\text{O}_7\text{F}$ (15), representing $n = 2$ and $n = 3$ in the homologous series M_nX_{3n-1} . If the structure contains two sets of crystallographic shear planes intersecting each other a so-called block structure is formed, which contains columns of ReO_3 type. These columns or blocks are directly interconnected by edge-sharing between component octahedra along the CS planes.

$\text{Pb}_2\text{Nb}_3\text{O}_7\text{F}_5$ (1) is so far the only known member, with $n = 3$, of a hypothetical homologous series $\text{Pb}_2\text{F}_2\text{Nb}_n\text{O}_{2n+1}\text{F}_n$. It is closely related to the so called Aurivillius phases, $\text{Bi}_2\text{O}_2\text{A}_{n-1}\text{M}_n\text{O}_{3n+1}$ (16) but with lead replacing bismuth in the layers and with the perovskite A sites vacant. The A_2X_2 layers play a role in these structures somewhat similar to that of the CS planes in, e.g., $\text{Nb}_3\text{O}_7\text{F}$.

In the present structure, $\text{Pb}_{12}\text{Ta}_9\text{O}_{20}\text{F}_{29}$, two sets of intersecting " $\text{Pb}_2\text{F}_2^{2+}$ " layers separate the ReO_3 -type columns, and the structure could be regarded as an Aurivillius-type block structure analogous to the CS block structure phases. The analogy must not be carried too far, however. The CS block structures can tolerate a fairly large variation in the size of the columns,

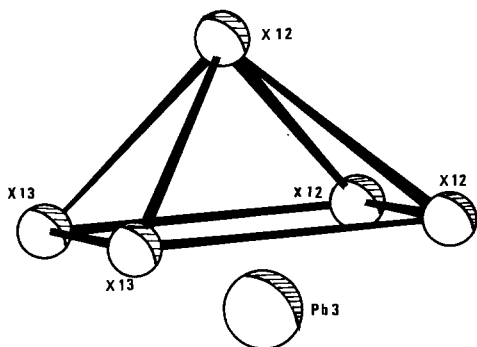


FIG. 2. The arrangement of F atoms about $\text{Pb}(3)$.

whereas the slight rotation of the columns in $\text{Pb}_{12}\text{Ta}_9\text{O}_{20}\text{F}_{29}$, necessary to accommodate the lead atoms in the " $\text{Pb}_2\text{F}_2^{2+}$ " layers, causes a mismatch between the layers at the intersection, a mismatch that varies with the size of the blocks. It is quite possible that the arrangement of the $\text{Pb}(3)$ atoms in $\text{Pb}_{12}\text{Ta}_9\text{O}_{20}\text{F}_{29}$ is the only favorable way to relax this mismatch and that this is the reason why efforts to synthesize compounds of this type with other sizes of the blocks have hitherto been unsuccessful.

Acknowledgments

I express my gratitude to Dr. M. Lundberg and Professor A. Magnéli for many stimulating discussions and for their encouraging interest in this work. I am also indebted to Dr. W. Sahle for his skillful help with the electron microscopy investigation. I also thank Professor L. Kihlberg for his valuable comments on this manuscript.

References

1. Ö. SÄVBORG, *J. Solid State Chem.* **57**, 143 (1985).
2. Ö. SÄVBORG, *J. Solid State Chem.* **57**, 148 (1985).
3. Ö. SÄVBORG, *J. Solid State Chem.* **57**, 160 (1985).
4. P. G. HAMBLING, *Acta Crystallogr.* **6**, 98 (1953).
5. *International Tables for X-ray Crystallography*, Vol. IV, Kynoch Press, Birmingham (1974).
6. Ö. SÄVBORG AND M. LUNDBERG, *J. Solid State Chem.* **57**, 135 (1985).
7. I. D. BROWN AND KANG KUN WU, *Acta Crystallogr. B* **32**, 1957 (1976).
8. L. K. FREVELL AND H. W. RINN, *Acta Crystallogr.* **9**, 626 (1956).
9. R. D. BURBANK AND F. N. BENSEY, *J. Chem. Phys.* **27**, 982 (1957).
10. R. D. BURBANK AND G. R. JONES, *Inorg. Chem.* **13**, 1071 (1974).
11. R. D. BURBANK AND G. R. JONES, *J. Amer. Chem. Soc.* **96**, 43 (1974).
12. R. J. GILLESPIE AND R. S. NYHOLM, *Q. Rev. Chem. Soc.* **11**, 339 (1957).
13. W. J. MOORE AND L. PAULING, *J. Amer. Chem. Soc.* **63**, 1392 (1941).
14. R. J. GRUEHN, *J. Less-Common Met.* **11**, 119 (1966).
15. S. ANDERSSON, *Acta Chem. Scand.* **18**, 2334 (1964).
16. B. AURIVILLIUS, *Ark. Kemi* **2**, 519 (1950–1951).